Improvement of Algorithm for Quantification of Regional Myocardial Blood Flow Using ^{15}O-Water with PET

Chietsugu Katoh, MD[1,2]; Koichi Morita, MD[3]; Tohru Shiga, MD[3]; Naoki Kubo, MD[2]; Kunihiro Nakada, MD[3]; and Nagara Tamaki, MD[3]

[1]Department of Tracer Kinetics, Hokkaido University School of Medicine, Sapporo, Japan; [2]Department of Health Science, Hokkaido University School of Medicine, Sapporo, Japan; and [3]Department of Nuclear Medicine, Hokkaido University School of Medicine, Sapporo, Japan

^{15}O-Water and dynamic PET allow noninvasive quantification of myocardial blood flow (MBF). However, complicated image analyzing procedures are required, which may limit the practicality of this approach. We have designed a new practical algorithm, which allows stable, rapid, and automated quantification of regional MBF (rMBF) using ^{15}O-water PET. We designed an algorithm for setting the 3-dimensional (3D) region of interest (ROI) of the whole myocardium semiautomatically. Subsequently, a uniform input function was calculated for each subject using a time–activity curve in the 3D whole myocardial ROI. The uniform input function allows the mathematically simple and robust algorithm to estimate rMBF. **Methods:** Thirty-six volunteers were used in the static ^{15}O-CO and dynamic ^{15}O-water PET studies. To evaluate the reproducibility of the estimates, a repeated ^{15}O-water scan was obtained under resting condition. In addition, to evaluate the stability of the new algorithm in the hyperemic state, a ^{15}O-water scan was obtained with adenosine triphosphate. This algorithm includes a procedure for positioning a 3D ROI of the whole myocardium from 3D images and dividing it into 16 segments. Subsequently, the uniform input function was calculated using time–activity curves in the whole myocardial ROI and in the LV ROI. The uniform input function allowed this simple and robust algorithm to estimate the rMBF, perfusable tissue fraction (PTF), and spillover fraction (Va) according to a single tissue compartment model. These estimates were compared with those calculated using the original method. A simulation study was performed to compare the effects of errors in PTF or Va on the MBF using the 2 methods. **Results:** The average operating time for positioning a whole myocardial ROI and 16 regional myocardial ROIs was <5 min. The new method yielded less deviation in rMBF (0.876 ± 0.177 mL/min/g, coefficient of variation [CV] = 20.2%, n = 576) than those with the traditional method (0.898 ± 0.271 mL/min/g, CV = 30.1%, n = 576) ($P < 0.01$). In the hyperemic state, the new method yielded less deviation in rMBF (3.890 ± 1.250 mL/min/g, CV = 32.1%) than those with the traditional method (3.962 ± 1.762 mL/min/g, CV = 44.4%) ($P < 0.05$). This method yielded significantly higher reproducibility of rMBF (r = 0.806, n = 576) than the original method (r = 0.756, n = 576) ($P <$ 0.05). Our new method yielded a better correlation in the repeated measurement values of rMBF and less variability among the regions in the myocardium than with the original theory of the ^{15}O-water technique. The simulation study demonstrated fewer effects of error in the PTF or Va on the MBF value with the new method. **Conclusion:** We have developed a technique for an automated, simplified, and stable algorithm to quantify rMBF. This software is considered to be practical for clinical use in myocardial PET studies using ^{15}O-water with a high reproducibility and a short processing time.

Key Words: myocardial blood flow; ^{15}O-water; PET

J Nucl Med 2004; 45:1908–1916

Previous animal and clinical studies with ^{15}O-water and PET have shown the feasibility of quantitative estimates of regional myocardial blood flow (rMBF) (*1–4*). The use of ^{15}O-water PET provides a noninvasive method for in vivo quantification of rMBF, perfusable tissue fraction (PTF), and spillover fraction (Va). However, the original method requires complicated image analyzing procedures, which may limit the practicality of this approach. A crucial limitation of the original method is the manual positioning of regional myocardial regions of interest (ROIs). It is a very time-consuming procedure, especially when the operator is required to set the same myocardial ROIs on the paired rest and stress studies. The manual approach remains operator dependent. Moreover, in the original algorithm, the input function is estimated using the time–activity curves in the regional myocardial ROI and in the left ventricular (LV) ROI (*5,6*). When the input function is derived from the regional myocardial time–activity curve, it would not be uniform for each regional myocardium in each subject (*5*). We accessed the new algorithm using a uniform input function, which may improve the stability and reproducibility of the estimates.

Several automatic algorithms are reported for setting the myocardial ROI in myocardial SPECT studies (*7–9*);

Received Jan. 23, 2004; revision accepted Jun. 3, 2004.

For correspondence or reprints contact: Chietsugu Katoh, MD, Department of Tracer Kinetics, Hokkaido University School of Medicine, N-15, W-7, Kita-ku, Sapporo, Hokkaido, Japan 060-8638.

E-mail: chtgkato@med.hokudai.ac.jp

The algorithms permit short operating time as well as operator-independent and robust results. For ^{15}O-water myocardial PET studies, we attempted the same approach. In this study, we developed a software algorithm, which allows rapid, stable, and automated estimation of the rMBF. We put particular emphasis on the performance of the software to achieve practical analysis times for clinical deployment.

MATERIALS AND METHODS

We designed an algorithm for setting the 3-dimensional (3D) ROI of the whole myocardium and dividing it into 16 segments automatically, overcoming the difficulty of the process, which is significantly time consuming if it is performed manually. Subsequently, a uniform input function was calculated for each subject using time–activity curves in the whole myocardial ROI and in the LV ROI. The uniform input function allows the mathematically simple and robust algorithm to estimate rMBF, PTF, and Va. These estimates were compared with those calculated with the original method.

Subjects

Thirty-six healthy volunteers (34 men, 2 women; mean age, 29.9 ± 8.6 y) were studied in Hokkaido University Medical Hospital. Data acquisitions were performed as a prospective study. All subjects had normal laboratory tests and no symptoms or history of cardiovascular disease. Heart rates and end-systolic and end-diastolic blood pressures were continuously monitored and recorded. The nature, purpose, and potential risks of the study were explained to all subjects before they gave their voluntary consent to participate. The study was approved by the ethical committee of Hokkaido University Medical Hospital.

Production of ^{15}O-CO and ^{15}O-Water

For the production of ^{15}O-labeled compounds, a low-energy deuteron accelerator was used (CYPRIS-HM18; Sumitomo Heavy Industries). ^{15}O-Water was produced with a dialysis technique in a continuously working water module. Sterility and pyrogen tests were performed daily to verify the purity of the product. Gas chromatographic analysis was performed to verify the purity of the product before each study.

Image Acquisition

PET scans were obtained using an ECAT HR+ scanner (Siemens/CTI Corp.) equipped with ^{68}Ge/^{68}Ga retractable line sources for transmission scans. All emissions and transmissions were acquired in the 2-dimensional mode and reconstructed using filtered backprojection with a Hanning filter (cutoff, 0.4). The in-plane resolution was 6.2-mm full width half maximum in a 128 × 128 matrix image. All data were corrected for dead time, decay, and measured photon attenuation.

The optimal imaging position was determined by a 1-min rectilinear scan. A 5-min transmission scan was then acquired for the purpose of attenuation correction of all subsequent emission scans.

A blood-pool scan was obtained in the following manner. Each subject's nostrils were closed and he or she inhaled ^{15}O-CO (0.14% CO mixed with room air) for 1 min. After inhalation of the tracer, a period of 3 min was allowed for the CO to combine with hemoglobin before a 5-min static scan was started. During the 5-min scan period, venous blood samples were drawn every 2 min, and the concentration of radioactivity in whole blood was measured with an automatic γ-counter (ARC-400; ALOKA Inc.). The inhaled dose in the CO examination was 2,000 MBq.

^{15}O radioactivity returned to background levels 10 min after the blood-pool scan. ^{15}O-Water was infused into an antecubital vein as a slow (2 min) infusion. The administrated dose of ^{15}O-water was 500 MBq/min. A 20-frame dynamic PET scan, consisting of 6 × 5 s, 6 × 15 s, and 8 × 30 s frames, was acquired for 6 min.

After allowing a further 10 min for decay, another dynamic scan using ^{15}O-water was acquired. Fifteen minutes later, adenosine triphosphate (ATP) was infused for 7 min at 0.16 mg/kg/min. A 20-frame dynamic ^{15}O-water PET scan was started 2 min after the beginning of ATP infusion. Blood pressure and heart rate were recorded before each scanning.

Data Processing

Original coincidence data were stored as sinograms and then normalized, corrected for attenuation, and backprojected in a dedicated array processor to obtain the final images. The analysis of PET images was accomplished using an image analysis package (Dr. View; Asahi-Kasei) and software developed in our institute by use of programming language C.

Processing Blood Volume Images. Functional blood volume images were created by dividing the ^{15}O-CO PET counts by the blood sample counts measured in the cross-calibrated well counter. ^{15}O-Water washout images were calculated by subtracting the blood volume images from the sum of the ^{15}O-water dynamic images (*10*).

Calculation of Extravascular Density Images. The reconstructed transmission data were normalized on a pixel-by-pixel basis to the activity pixel counts in a ROI in the LV chamber of the transmission image and the density of blood. The extravascular images were calculated by subtracting the vascular components from the normalized transmission images using the blood volume images (*10*).

ROI Definition

Short axial blood volume images were generated semiautomatically, rotating horizontal and vertical long axial blood volume images (Fig. 1). This process was performed to define the heart long axis. This program generates short axial ^{15}O-water dynamic images and extravascular density images automatically, with the same rotation angles used in the blood volume images.

The short axial blood volume images were used to define the ROI in the left ventricle, showing 85% recovery of the true blood tracer concentration (*11*) (Fig. 2). Early-phase short axial ^{15}O-water images were calculated by summing first the 2-min dynamic images. A linear 6-parameter registration (*12*) was performed for registration of the ^{15}O-water images to the ^{15}O-CO images. Short axial ^{15}O-water washout images were generated calculating the mean counts from 180- to 300-s frame images.

When the ^{15}O-water washout images were superimposed on extravascular images and analyzed with a semiautomated edge-detection routine, a whole myocardial ROI was determined. The program is designed to extract a 3D region enclosing the whole myocardial wall. The process is performed in the 3D matrices. At first, the apical and basal portion (valve plane) are pointed manually. The activity distribution of the midventricular and basal portions is expressed in circular cylindric coordinates relative to the heart long axis, assuming a shape of the heart that resembles a

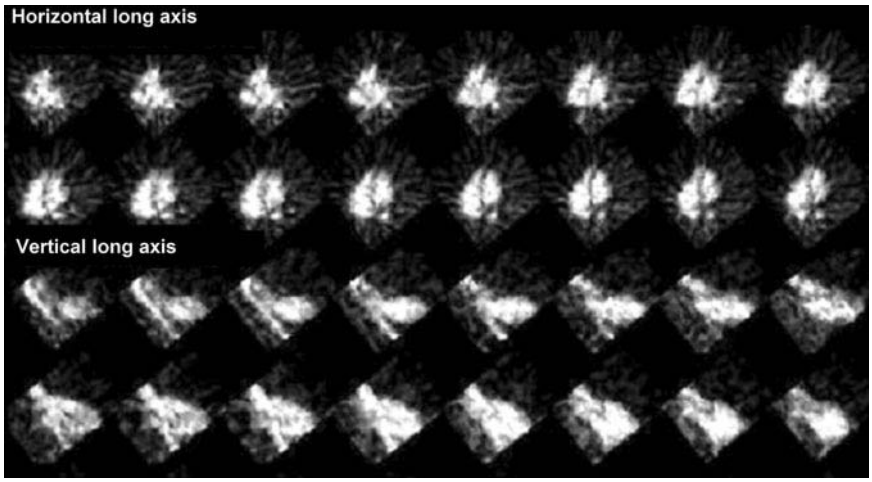

FIGURE 1. Transaxial ^{15}O-CO images were rotated to generate short axial images in horizontal long axial and in vertical axial slices. Rotation angles for each reorientation were set manually monitoring the rotated images.

hemisphere in the apex and a cylindroid in the midventricular and basal portions. For each possible ray in a radial direction from the heart long axis, the first crossing of a given activity threshold (e.g., 60%) is detected and every point farther than the maximal possible wall thickness (e.g., 2 cm) is excluded from calculation (*13*). Then, a $3 \times 3 \times 3$ 3D smoothing filter is applied to the edge of the ROI, and a bullet-shaped ROI that encloses the whole myocardium is generated (Fig. 3A). Regional myocardial ROIs were positioned automatically in 16 anatomic segments according to the rule in the American Society of Echocardiography report (*14*) (Fig. 3B).

The LV time–activity curve was generated with the LV ROI and dynamic ^{15}O-water data. The whole and regional myocardial tissue time–activity curves were generated with these myocardial ROIs and dynamic ^{15}O-water data.

Original Method for Estimation of rMBF

A conventional theory to estimate rMBF using ^{15}O-water is described by the following equation for a single tissue compartment model (Fig. 4A):

$$dCt(t)/dt = F \cdot Ca(t) - (F/p) \cdot Ct(t), \qquad \text{Eq. 1}$$

where Ca(t) is the concentration of ^{15}O-water in arterial whole blood (cps/mL), Ct(t) is the concentration of ^{15}O-water in myocardial tissue (cps/g), F is rMBF (mL/g/min), and p is the partition coefficient of water in the myocardium (0.91 mL/g), respectively.

The concentration of radioactivity in the LV ROI, LV(t), is expressed as follows:

$$LV(t) = \beta \cdot Ca(t) + (1 - \beta) \cdot \rho \cdot Ct(t), \qquad \text{Eq. 2}$$

where ρ is a myocardial tissue density (1.04 g/mL), and β corresponds to a recovery coefficient of the LV ROI concentration. The value of β is calculated using the ^{15}O-CO blood volume scan as follows (*6*): β = LV ROI counts in the ^{15}O-CO blood volume scan (cps/mL)/sampled blood counts during the ^{15}O-CO scan (cps/g)/whole blood density (1.06 g/mL)

The measured tissue time–activity curve in a regional myocardial ROI, R(t) is described by:

$$R(t) = PTF \cdot Ct(t) + Va \cdot Ca(t), \qquad \text{Eq. 3}$$

where PTF is the grams of perfusable tissue per 1 mL of myocardial ROI (g/mL) and Va is the arterial blood volume in the myocardial ROI and spillover from the left ventricle into the myocardial ROI (mL/mL).

The values of PTF, Va, and F are estimated by Equations 1–3 with a nonlinear least-squares regression analysis.

Modified Method for Estimation of rMBF

In the modified method in this study, we have developed a simplified algorithm (Fig. 4B). First, a uniform input function

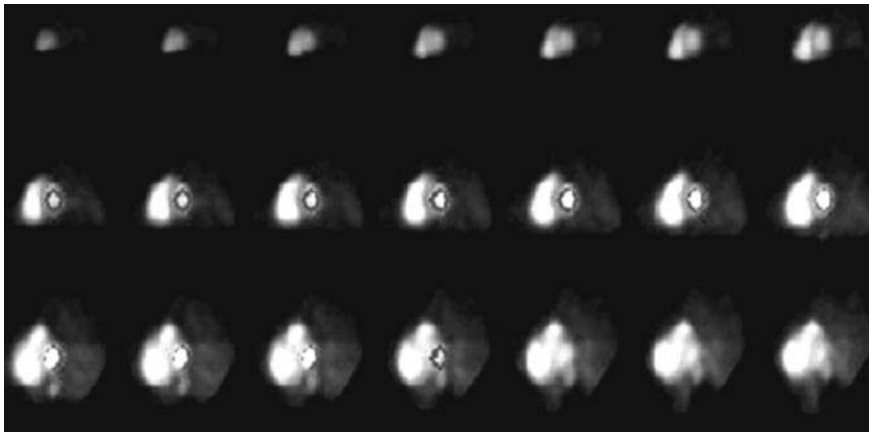

FIGURE 2. Positioning of LV ROI on short axial ^{15}O-CO images. When a position in left ventricle is clicked on the image, the LV ROI is set automatically. Program defines mean ROI count yields as 85% of the true blood volume concentration.

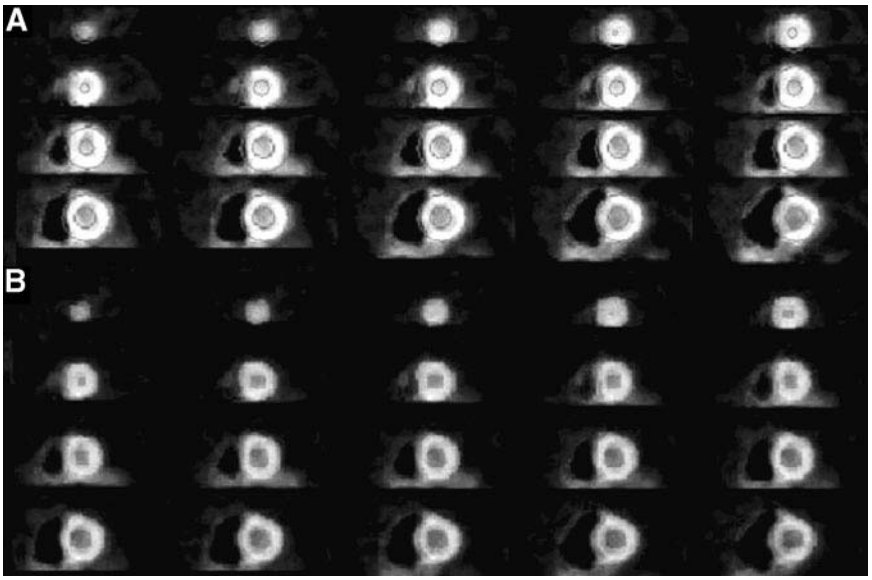

FIGURE 3. When ^{15}O-water washout images are superimposed on extravascular images and analyzed with semiautomated edge-detection routine, a whole myocardial ROI is determined. Program extracts 3D region enclosing the whole myocardial wall; process is performed in the 3D matrices. Positioning of whole LV wall ROI on ^{15}O-water washout images is evident. (A) Circles are placed semiautomatically inside and outside myocardial edges. (B) Program defines endocardial and epicardial borders of LV wall (B).

$Ca^{whole}(t)$ was derived using a whole myocardial ROI curve with the original method. When the values of PTF, Va, and F for a whole myocardial ROI were determined by the non–least-squares method, the input function curve $Ca^{whole}(t)$ was calculated by Equations 1–3. Then, the following equations were used to determine the values of PTF, Va, and F for the regional myocardium with a nonlinear least-squares method:

$$dCt(t)/dt = F \cdot Ca^{whole}(t) - (F/p) \cdot Ct(t). \quad \text{Eq. 4}$$

$$R(t) = PTF \cdot Ct(t) + Va \cdot Ca^{whole}(t). \quad \text{Eq. 5}$$

The following 4 sets of rMBF in each segment in the myocardial wall were estimated for each subject:

- Original rMBF1 was calculated using the first ^{15}O-water dynamic data with a conventional method.
- Original rMBF2 was calculated using the second ^{15}O-water dynamic data with a conventional method.
- Modified rMBF1 was calculated using the first ^{15}O-water dynamic data with a modified method.
- Modified rMBF2 was calculated using the second ^{15}O-water dynamic data with a modified method.

In addition, stability of rMBF in the hyperemic state was estimated for each subject:

- Original rMBF was calculated using hyperemic ^{15}O-water dynamic data with a conventional method.
- Modified rMBF was calculated using hyperemic ^{15}O-water dynamic data with a modified method.

Estimates (MBF, PTF, and Va) in the apical, anterior, septal, inferior, and lateral wall were calculated from apical, middle, and basal regions as shown in Figure 5A. Our new program presents rMBF on the polar map and on ^{15}O-water images (Fig. 5B). When paired rest and stress studies are performed, our program presents rMBF at rest, rMBF in the hyperemic state, and coronary flow reserve in each region on the polar maps (Fig. 6).

Statistical Analysis

To evaluate the reproducibility of the results, Pearson correlation coefficients were calculated and a Bland–Altman plot was applied for rMBF derived from a traditional method (Original rMBF1 vs. Original rMBF2) and from a modified method (Modified rMBF1 vs. Modified rMBF2). The differences in these cor-

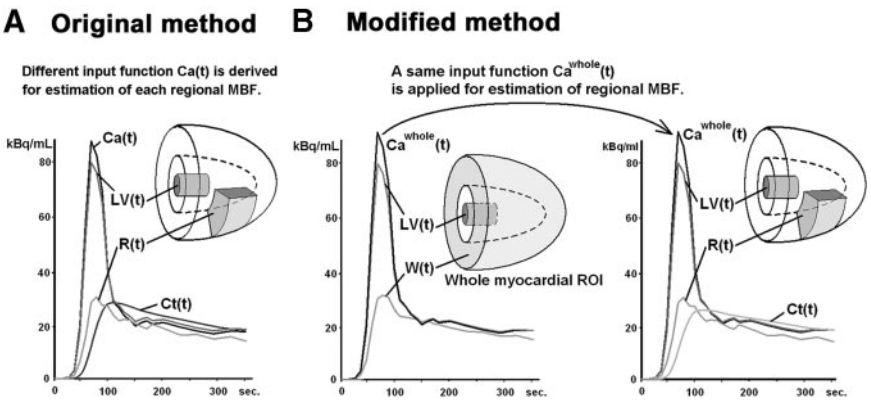

FIGURE 4. Scheme of algorithm of original method (A) and modified method (B). (A) R(t) and LV(t) correspond to measured time–activity curves in regional myocardial ROI and in left ventricle, respectively. Input function Ca(t), tissue time–activity curve Ct(t), and rMBF are derived from R(t) and LV(t). (B) W(t) corresponds to measured time–activity curve in whole myocardial ROI. Uniform input function $Ca^{whole}(t)$ is derived from W(t) and LV(t). Then, each rMBF is estimated using a known input function $Ca^{whole}(t)$ and R(t).

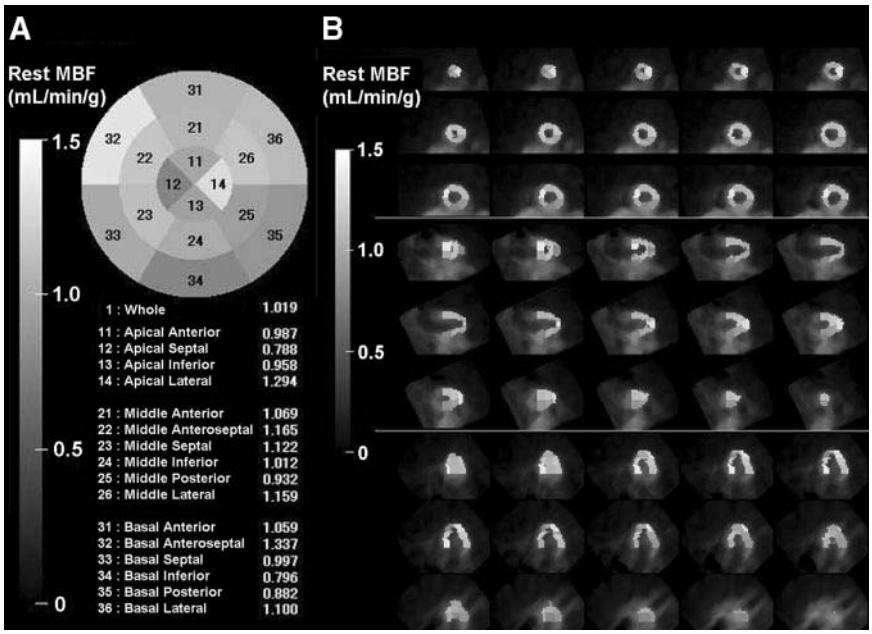

FIGURE 5. Program automatically divides whole myocardial ROI into 16 anatomic segments according to the rule in the American Society of Echocardiography report (*14*). Quantified rMBF values are presented automatically on polar map (A) and on ^{15}O-water images (B).

relation coefficients were compared using Fisher *z*-transformation. To evaluate the regional variability of the estimates (MBF, PTF, and Va), paired Student *t* tests were performed to examine the difference between the original and modified methods. The χ^2 test was performed to evaluate the differences in the variation of each estimate. All data are presented as mean ± SD. $P < 0.05$ is considered to be statistically significant in assessing the differences of correlation coefficients and differences of variability.

Simulation Study

A simulation study was performed to assess the effects of errors in the measurement of PTF or Va on the calculated value of MBF in the original and modified methods.

The mean myocardial and LV time–activity curves were generated using data of the 36 subjects. The percentage error in MBF was calculated when the percentage error of the PTF or Va was changed from −10% to +10%.

RESULTS

The variables of systolic pressure, diastolic pressure, and heart rate in the first and second ^{15}O-water dynamic scans were 105.3 ± 8.4 and 105.9 ± 9.1 mm Hg, 54.7 ± 7.7 and 53.4 ± 8.8 mm Hg, and 60.3 ± 8.5 and 60.8 ± 7.3 beats/min, respectively. No significant hemodynamic change was observed during the 2 dynamic acquisitions. In the hyperemic state, the variables of systolic pressure, diastolic pressure, and heart rate were 103.6 ± 9.5 mm Hg, 52.1 ± 8.7 mm Hg, and 87.2 ± 8.4 beats/min.

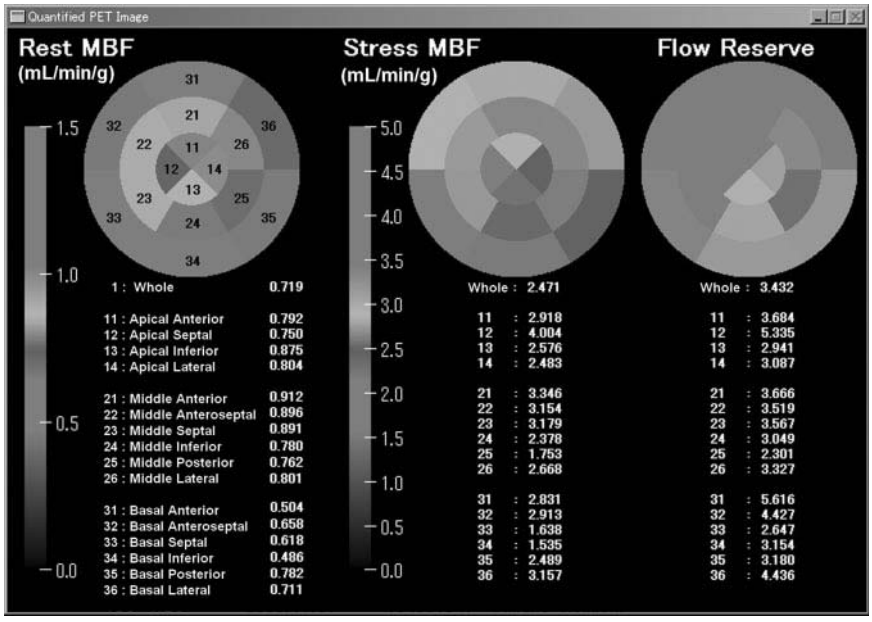

FIGURE 6. When paired rest and stress studies are performed, the new program generates automatically polar maps of rest MBF, stress MBF, and coronary flow reserve.

TABLE 1
Comparison of rMBF, PTF, and Va in Resting State Between Original and Modified Methods

Region	rMBF (mL/min/g)		PTF (g/mL)		Va (mL/mL)	
	Original	Modified	Original	Modified	Original	Modified
Among subjects						
Apical	1.011 ± 0.443	0.960 ± 0.310*	0.581 ± 0.101	0.577 ± 0.102*	0.267 ± 0.117	0.270 ± 0.118*
Anterior	1.071 ± 0.298	1.018 ± 0.216*	0.538 ± 0.084	0.533 ± 0.085*	0.329 ± 0.084	0.333 ± 0.084*
Septal	0.845 ± 0.282	0.843 ± 0.218	0.532 ± 0.133	0.527 ± 0.138	0.473 ± 0.134	0.481 ± 0.136
Inferior	0.801 ± 0.181	0.808 ± 0.159	0.641 ± 0.138	0.642 ± 0.140	0.307 ± 0.125	0.307 ± 0.126
Lateral	0.946 ± 0.224	0.928 ± 0.187*	0.576 ± 0.104	0.574 ± 0.105*	0.271 ± 0.080	0.273 ± 0.080*
Total†	0.898 ± 0.271	0.876 ± 0.177*	0.588 ± 0.107	0.584 ± 0.110*	0.322 ± 0.134	0.325 ± 0.136*
Within a subject						
Total‡	0.906 ± 0.295	0.886 ± 0.193*	0.590 ± 0.149	0.551 ± 0.101*	0.337 ± 0.144	0.352 ± 0.116*

*$P < 0.05$.
†$n = 576$.
‡$n = 36$.

The average analysis time to define a whole myocardial ROI and 16 regional myocardial ROIs was <5 min. With the conventional manual ROI setting program, it took >30 min. The use of the algorithm for defining ROIs resulted in the decrease of the analysis time. After positioning a whole myocardial ROI and 16 regional myocardial ROIs, the procedure to estimate these rMBFs took only a few seconds with both the original and our modified methods.

Table 1 shows a comparison of the variables of rMBF, PTF, and Va at rest in the various regions of the myocardium among subjects and within a subject. The modified method yielded less deviation and a lower rMBF than those with the traditional method. The apical, anterior, and lateral regions showed a significant decrease in rMBF. The modified method yielded a lower PTF than those with the original method. The apical, anterior, and lateral regions showed a significant decrease in PTF. The simplified method yielded a higher Va than those with the traditional method. The apical, anterior, and lateral regions yielded a significant increase in Va. Significant differences and less deviation of these estimates in the resting condition were presented within a subject between the original and modified methods.

Table 2 presents a comparison of the variables of the measurement of rMBF in the hyperemic state among subjects. The new method yielded less deviation in rMBF (3.890 ± 1.250 mL/min/g, coefficient of variation [CV] = 32.1%) than those with the traditional method (3.962 ± 1.762 mL/min/g, CV = 44.4%) ($P < 0.05$) in the hyperemic condition. Significant differences and less deviation of these estimates in the hyperemic condition were presented within a subject between the original and modified methods.

Figure 7 shows plots of the correlations between rMBF calculated from the first and second ^{15}O-water dynamic scans using the original method and the modified algorithm. The modified method yielded significantly higher reproducibility than the original method ($P < 0.05$). The Bland–Altman test shows better reproducibility with the modified method.

Figure 8 shows the results of the simulation studies, which demonstrated the error of the PTF or the Va propagated to the measured value of MBF with a simplified method or a modified method. Fewer errors in the estimated MBF were induced by errors in the PTF or the Va with a modified method. In the original algorithm, an overestimation of 10% in the PTF caused an overestimation of approximately 28% in MBF, whereas, in the modified algorithm, the overestimation was suppressed 20% in MBF. In the original algorithm, an underestimation of 10% in the Va caused an overestimation of approximately 26% in MBF, whereas in the modified algorithm, the overestimation was suppressed 20% in MBF.

DISCUSSION

In this study, we designed a software algorithm for setting the 3D ROI of the whole myocardium and dividing it into 16 regions automatically with a clinically acceptable processing time. At the same time, the software was equipped

TABLE 2
Comparison of rMBF (mL/min/g) in Hyperemic State Between Original and Modified Methods

Region	Original	Modified
Among subjects		
Apical	4.234 ± 1.834	4.017 ± 1.411*
Anterior	4.160 ± 1.799	4.059 ± 1.328*
Septal	3.785 ± 1.489	3.674 ± 1.236*
Inferior	3.613 ± 1.303	3.569 ± 1.159*
Lateral	4.072 ± 1.622	3.953 ± 1.174*
Total†	3.962 ± 1.762	3.890 ± 1.250*
Within a subject		
Total‡	3.985 ± 1.521	3.801 ± 1.308*

*$P < 0.05$.
†$n = 576$.
‡$n = 36$.

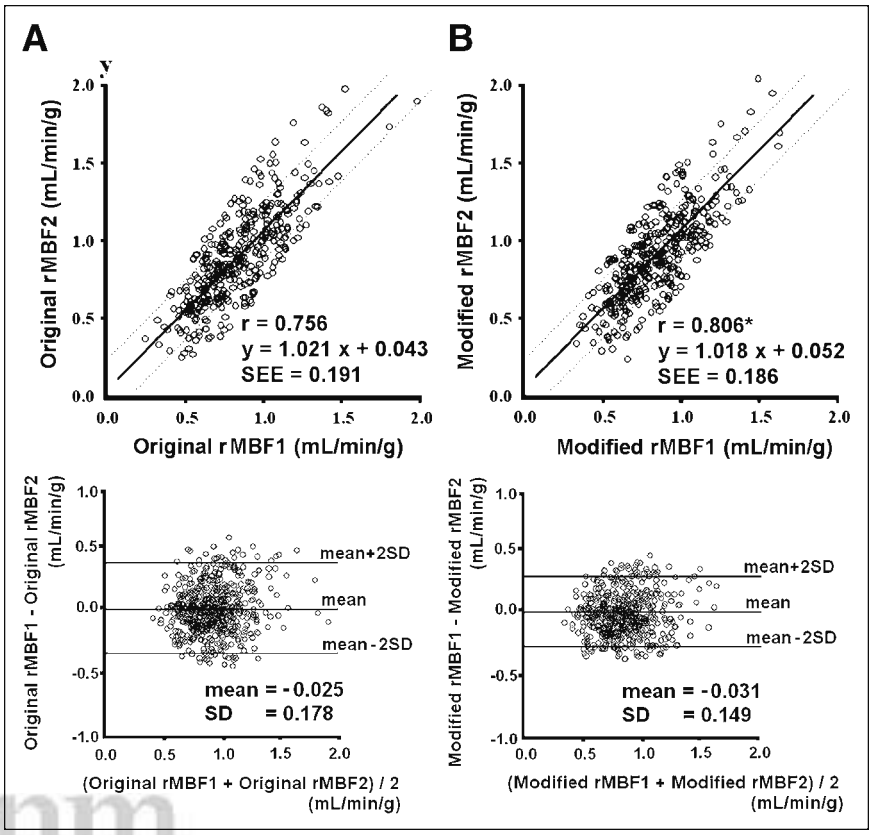

FIGURE 7. Reproducibility of rMBF with original method (A) and modified algorithm (B) in 576 ROIs of 36 subjects. (Top) Regression lines and intervals of SEEs are drawn. Correlation was significantly higher when calculated with modified method than with original method ($P < 0.05$). (Bottom) Bland–Altman plots.

with a simplified algorithm to calculate MBF using a uniform input function for each region for stable estimation.

We designed an algorithm for setting the 3D ROI of the whole myocardium and dividing it into 16 segments automatically, overcoming the difficulty of the process, which is significantly time consuming if it is performed manually. At the present time, our ROI setting software requires manual handling of a few processes, but it enables ROI definition almost independently of the operator and allows stable rMBF quantification. Various approaches are used for automatic 3D delineation of the LV myocardium in myocardial SPECT studies (*15–17*). However, it might be difficult to apply these algorithms for ^{15}O-water PET data, because the PET studies performed with ^{15}O-labeled tracers yield less delineated and less homogeneous images than SPECT studies. We designed a simple method for positioning a 3D ROI, which covers the whole LV myocardium. For estimating rMBF with ^{15}O-water PET, is not necessary to set a tight ROI tracing the contours of the myocardium (*18*).

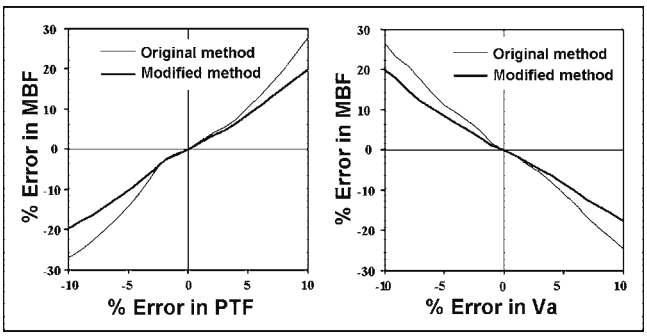

FIGURE 8. Simulations demonstrate the effect of error in PTF or Va in calculated MBF values. In estimated MBF, fewer errors were induced by errors in PTF or Va with modified method than with original method.

To improve the reproducibility and stability of quantitative measurements of the rMBF, we applied a uniform input function for each region. Our modified method yielded a better correlation in the repeated measurement values of rMBF and less variability among the regions in the myocardium than with a conventional theory of the ^{15}O-water technique. Also, in the hyperemic state, the new method yielded less deviation in rMBF than those with the original method. A simulation study also showed that the modified algorithm yielded fewer errors in the estimated MBF.

The main reason for the better reproducibility and stability in the modified method is explicable. In the original method, a nonlinear least-squares method is used to determine 3 unknown values (PTF, Va, and MBF) and 2 unknown curves (Ca(t), Ct(t)) by fitting 2 curves (PTF Ct(t) + VaCa(t) and βCa(t) + (1 − β)ρCt(t)) to the 2 known curves (R(t) and LV(t)), respectively. The value (1 − β) is the contribution ratio of the whole myocardial radioactivity (*6*); it is an anatomic parameter for a whole LV myocardium. The equation LV(t) = βCa(t) + (1 − β)ρCt(t) should be

applied to the whole myocardial data. When the value (1 − β) is applied to estimate regional myocardial data, the contribution ratio must be overestimated. Then the original method might overestimate rMBF and underestimate the regional spillover fraction (Va).

Our present study demonstrated that the original method yielded significantly higher rMBF and a lower Va than the modified method, especially in the apical, anterior, and lateral regions. In these regions, Va is overestimated in the conventional method.

To improve the stability of quantitative measurement of rMBF, we designed a new modified algorithm. In the modified method, using the known curve $Ca^{whole}(t)$, the parameters (PTF, Va, and MBF) are derived by fitting only 1 curve (PTF Ct(t) + Va $Ca^{whole}(t)$) to the known curve R(t). This fitting is mathematically simplified and more stable to estimate the parameters than that in the original algorithm.

The simulation study indicated that the modified method showed fewer effects of error in the PTF and the Va on the MBF compared with the original method.

Theoretically, whole myocardial ROI data are recommended to derive an input function (*11*); it was difficult to determine a whole myocardial ROI because the procedure requires a 3D ROI setting technique. In this study, we have developed a new program for the procedure that overcame the difficulty of positioning the whole myocardial ROI. We developed a new algorithm to improve the stability of the estimates calculated from ^{15}O-water PET; however, it is also essential to improve the reconstruction method for achieving better image quality using ^{15}O-water with PET (*19*).

The principal difficulty in validating the new approach is the lack of a gold standard to determine the success of the algorithm. Therefore, we relied primarily on the improvement of reproducibility and the decrease in the variability of MBF among the regions in the myocardium. We confirmed these results and appropriate values of estimates (*20*).

In this study, we performed ^{15}O-CO scanning once in the protocol, which was not repeated before each ^{15}O-water PET scan. The ^{15}O-CO image is used only for positioning the LV ROI in our program, and each ^{15}O-water PET image is transferred appropriately with the registration algorithm. It is ideal to acquire an ^{15}O-CO image before every ^{15}O-water scan for precise ROI setting in the left ventricle. However, the algorithm to derive MBF in this study is equipped for estimating appropriate spillover in each myocardium (*5*); the estimated MBF with the present program might be robust enough to detect the subtle difference in the size or positioning of the LV ROI.

The limitation of this study is that we could not assess the reproducibility of measured rMBF in the hyperemic state. However, it was impossible to perform repeated ^{15}O-water PET studies with ATP because of ethical concerns. In the present study, we did not apply our new program to the patients with ischemic heart disease. Further clinical validations are needed.

At present, our program requires a ^{15}O-CO scan for estimation of MBF because this program is designed not only for calculating MBF but also for estimating extravascular tissue density and the PTF index in the myocardium (*11*). These parameters require ^{15}O-CO images. Recently, however, a new technique has been proposed for calculating MBF images directly from dynamic ^{15}O-water scans (*21–23*). When performing a PET study only for estimating MBF, our program should be equipped with the algorithm free from ^{15}O-CO scan.

CONCLUSION

We have developed a practical and automatic algorithm to quantify rMBF using ^{15}O-water with PET. This method includes a modified method, which is mathematically simplified and more stable than that in the original algorithm. This software yields desirable performance to achieve high reproducibility and practical computational times for clinical use in myocardial PET studies with ^{15}O-water.

REFERENCES

1. Bergmann SR, Fox RF, Rand AL, et al. Quantification of regional myocardial blood flow in vivo with $H_2{}^{15}O$. *Circulation.* 1984;70:724–733.
2. Knabb RM, Fox KAA, Sobel BE, et al. Characterization of the functional significance of subcritical coronary stenosis with $H_2{}^{15}O$ and positron emission tomography. *Circulation.* 1985;71:1271–1278.
3. Walsh MN, Bergmann SR, Steele RL, et al. Delineation of impaired regional myocardial perfusion by positron emission tomography with $H_2{}^{15}O$. *Circulation.* 1988;78:612–620.
4. Steven RB, Pilar H, Joanne M, et al. Noninvasive quantitation of myocardial blood flow in human subjects with oxygen-15-labeled water and positron emission tomography. *J Am Coll Cardiol.* 1989;14:639–652.
5. Iida H, Kanno I, Takahashi A, at al. Measurement of absolute myocardial blood flow with $H_2{}^{15}O$ and dynamic positron emission tomography: strategy for quantification in relation to the partial-volume effect. *Circulation.* 1988;78:104–115.
6. Iida H, Rhodes CG, Silva R, et al. Use of the left ventricular time-activity curve as a noninvasive input function in dynamic oxygen-15-water positron emission tomography. *J Nucl Med.* 1992;33:1669–1677.
7. Germano G, Kavanagh PB, Waechter P, et al. A new algorithm for the quantification of myocardial perfusion SPECT. I. Technical principles and reproducibility. *J Nucl Med.* 2000;41:712–719.
8. Sharir T, Germano G, Waechter P, et al. A new algorithm for the quantification of myocardial perfusion SPECT. II. Validation and diagnostic yield. *J Nucl Med.* 2000;41:720–727.
9. Cachin F, Lipiecki J, Mestas D, et al. Preliminary evaluation of a fuzzy logic-based automatic quantitative analysis in myocardial SPECT. *J Nucl Med.* 2003; 44:1625–1632.
10. Iida H, Rhodes CG, Araujo LI, et al. Noninvasive quantification of regional myocardial metabolic rate for oxygen by use of $^{15}O_2$ inhalation and positron emission tomography: theory, error analysis, and application in humans. *Circulation.* 1996;94:792–807.
11. Iida H, Rhodes CG, Silva R, et al. Myocardial tissue fraction: correlation for partial volume effects and measure of tissue viability. *J Nucl Med.* 1991;32: 2169–2175.
12. Hill DL, Batchelor PG, Holden M, et al. Algorithm for radiological image registration. *Phys Med Biol.* 2001;46:R1–R45.
13. Biedenstein S, Schafers M, Stegger L, et al. Three-dimensional contour detection of left ventricular myocardium using elastic surfaces. *Eur J Nucl Med.* 1999;26: 201–207.
14. Henry WL. *Report of the American Society of Echocardiography, Committee on Nomenclature and Standards: Identification of Myocardial Wall Segments*. Raleigh, NC: American Society of Echocardiography; 1982.
15. Goris ML, McKillop JH, Briandet PA. A fully automated determination of the left ventricular region of interest in nuclear angiocardiography. *Cardiovasc Intervent Radiol.* 1981;4:117–123.
16. van Hastenberg RP, Kemerrink GJ, Hasman A. On the generation of short-axis

and radial long-axis slices in thallium-201 myocardial perfusion single-photon emission tomography. *Eur J Nucl Med.* 1996;23:924–931.
17. Faber TL, Cooke CD, Peifer JW, et al. Three-dimensional displays of left ventricular epicardial surface from standard cardiac SPECT perfusion quantification techniques. *J Nucl Med.* 1995;36:697–703.
18. Herrero P, Markham J, Myears DW, et al. Measurement of myocardial blood flow with positron emission tomography: correction for count spillover and partial volume effects. *Math Comput Model.* 1988;11:807–812.
19. Katoh C, Ruotsalainen U, Laine H, et al. A new iterative reconstruction method based on median root prior in quantification of myocardial blood flow and oxygen metabolism with PET. *J Nucl Med.* 1999;40:862–867.
20. Iida H, Yokoyama I, Agostini D, et al. Quantitative assessment of regional myocardial blood flow using oxygen-15-labelled water and positron emission tomography: a multicentre evaluation in Japan. *Eur J Nucl Med.* 2000;27:192–201.
21. Ahn JY, Lee MC, Kim SK, et al. Quantification of regional myocardial blood flow using dynamic $H_2{}^{15}O$ PET and factor analysis. *J Nucl Med.* 2001;42:782–787.
22. Schaefers KP, Spinks TJ, Camici PG, et al. Absolute quantification of myocardial blood flow with $H_2{}^{15}O$ and 3-dimensional PET: an experimental validation. *J Nucl Med.* 2002;43:1031–1040.
23. Kaufmann PA, Gnecchi-Ruscone T, Yap JT, et al. Assessment of the reproducibility of baseline and hyperemic myocardial blood flow measurements with ^{15}O-labeled water and PET. *J Nucl Med.* 1999;40:1848–1856.